Title
Integrated Design of Control Actuator Layer and Economic Model Predictive Control for Nonlinear Processes

Author
Durand, Helen Elaine

Publication Date
2014

Peer reviewed|Thesis/dissertation

UNIVERSITY OF CALIFORNIA

Los Angeles

Integrated Design of Control Actuator Layer and Economic Model Predictive Control for Nonlinear Processes

A thesis submitted in partial satisfaction of the requirements for the degree Master of Science in Chemical Engineering

by

Helen Elaine Durand

2014

ABSTRACT OF THE THESIS

Integrated Design of Control Actuator Layer
and Economic Model Predictive Control
for Nonlinear Processes

by

Helen Elaine Durand

Master of Science in Chemical Engineering
University of California, Los Angeles, 2014
Professor Panagiotis D. Christofides, Chair

In the present work, an economic model predictive control (EMPC) system is designed that accounts for the dynamics of the control actuators. A combined process-actuator dynamic model is developed to describe the process and control actuator dynamics and is used within the EMPC system. Integrating the design of the regulatory control layer, which controls the control actuators, and the supervisory control layer consisting of an EMPC system is an important consideration given the fact that EMPC may force an unsteady-state operating policy to optimize the process economics and the dynamics of the control actuator layer may affect the closed-loop process-actuator dynamics. Moreover, integral or average input constraints are often imposed within the EMPC solution. However, if the actuator layer is not accounted for in the EMPC system, the actuator output trajectory may not satisfy the integral input constraints. To address closed-loop stability of the combined process-actuator closed-loop system, stability constraints, designed via Lyapunov-based techniques, are imposed on the EMPC problem to guarantee closed-loop stability of the process system under the EMPC. An EMPC system accounting for the control actuator dynamics is applied to

a benchmark chemical process example to study the impact of the actuator dynamics on closed-loop economic performance and reactant material constraint satisfaction.

The thesis of Helen Elaine Durand is approved.

James Davis

Lieven Vandenberghe

Panagiotis D. Christofides, Committee Chair

University of California, Los Angeles

2014

Contents

List of Figures

List of Tables

ACKNOWLEDGEMENTS

I would like to thank my advisor Professor Panagiotis D. Christofides for his guidance and support throughout the course of the thesis.

I would like to thank Professor James Davis and Professor Lieven Vandenberghe for participating in my Master's thesis committee.

This work was submitted with the same title for publication in *Industrial & Engineering Chemistry Research* and is co-authored by Matthew Ellis and Professor Panagiotis D. Christofides. I would like to acknowledge the contributions of both of them to this thesis and express great thanks for their help.

Financial support from Aerojet Rocketdyne through the employee Tuition Assistance Program, and from the National Science Foundation and the Department of Energy, is gratefully acknowledged.

Chapter 1

Introduction

The chemical processing industry has long been interested in employing control methods that not only ensure stability and safety of a process, but that also force the process to achieve the highest profit possible. Currently, a hierarchical control structure is employed to accomplish these objectives. Real-time optimization (RTO) is used at the highest level of the hierarchy to compute the economically optimal operating point of the process system using a steady-state process model [1, 2]. Below RTO, the supervisory control layer receives the optimal operating point and uses it to compute control actions while accounting for process constraints and closed-loop performance considerations. Within chemical process industries, model predictive control (MPC) is widely implemented in the supervisory control layer and is typically formulated with a quadratic cost function (e.g., [3, 4, 5]). The MPC solution is used to provide set-points to the lower regulatory control layer, which often consists of a set of proportional-integral-derivative (PID) controllers. The regulatory control layer is responsible for dictating that the control actuators implement the control action requested by the supervisory control layer.

Within the context of MPC, the dynamics of the regulatory control layer and the control actuators are typically neglected and the dynamic model used within the MPC assumes that the control actuators can achieve an instantaneous response to the MPC computed control

actions. In practice, however, this may not be the case (e.g., [6]). Two main approaches have been used to address this issue: retuning the PID (regulatory) control layer to maintain the desired response to the MPC set-point changes, and accounting for actuator dynamics in the model predictive controller model.

PID tuning, re-tuning, and monitoring are used to address the first approach to dealing with the closed-loop actuator dynamics. A number of methods exist for tuning PID controllers such as the classical Ziegler-Nichols and Cohen-Coon tuning rules and internal model control (see, for example, [7, 8, 9, 10]) among many others. Because actuators may be poorly tuned or become poorly tuned over time as the process/actuator dynamics change, a variety of studies have been performed on methods for detecting poor tuning of PID control systems based on various performance metrics and then updating the controller tuning parameters (e.g., [11, 12, 13]). For example, case studies from the pulp and paper industry, where it is desirable to minimize disturbance effects, were used to examine some of the short-comings of an index based on minimum variances [11]. Performance indices were proposed for monitoring of set-point tracking and disturbance rejection, along with retuning methodologies when desired responses are not attained [12, 13]. Adaptive control methods to update PID parameters have also been explored (e.g., [14]). Some work explicitly considering MPC in the supervisory control layer and PID controllers in the regulatory control layer has also been carried out. For example, in [6], monitoring of process states is performed using exponentially weighted moving average residuals, and the PID controllers that manipulate the actuators to the MPC set-points are then automatically re-tuned for improved set-point tracking after the poor tuning is detected.

Another approach is to use a dynamic model in MPC that accounts for the control actuator dynamics. For example, the formulation and stability properties of an adaptive control allocation problem that explicitly accounts for the actuators is considered in [15]. In [16], an MPC that explicitly accounts for actuator dynamics is used to predict the optimal control allocation strategy for a re-entry vehicle and demonstrates improved tracking and

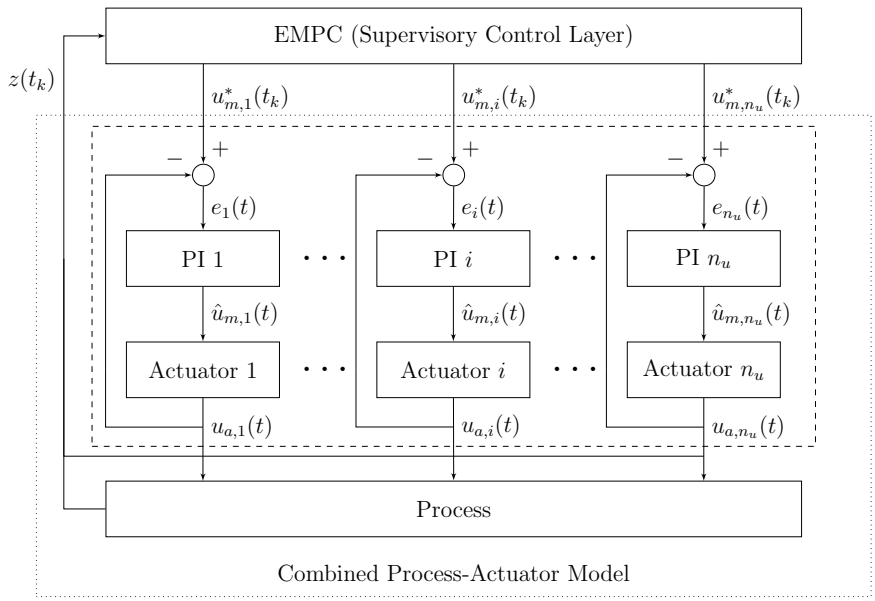

Figure 1.1: A block diagram of the control structure with EMPC at the supervisory control layer. The dashed box denotes the regulatory control and control actuator layer and consists of n_u actuators in closed-loop under PI controllers, and the dotted box represents the combined process-actuator model that will be developed for use in EMPC. The output of the PI controllers is denoted as $\hat{u}_{m,i}(t)$.

stability over a different method that does not include the actuator dynamics. In [17], a model of the actuator dynamics, which includes both actuator saturation and backlash, is incorporated in an MPC model. The resulting MPC demonstrated improved performance over the case where the actuator dynamics were not included in the MPC.

Recently, amid calls for tighter integration of process control and economic optimization, economic MPC (EMPC) has been proposed which is designed with a stage cost function that represents the process economics [18, 19, 20]. Thus, EMPC combines dynamic economic optimization and supervisory control. Because the EMPC cost function is not necessarily based on a desired steady-state, as is the standard MPC quadratic cost function, EMPC does not necessarily drive the system toward a steady-state. A number of EMPC formulations have been developed to deal with the resulting possibility of unsteady-state or dynamic operation (see the review paper [21] for an overview of recent developments on EMPC). Fig. 1.1 depicts a block diagram of the control architecture consisting of an EMPC system in

the supervisory control layer, the regulatory control layer (shown as a set of PI controllers), the control actuators, and the controlled process system.

To date, no work has been completed that examines the effect of actuator dynamics within the context of EMPC. Motivated by this, the present work considers developing an EMPC system that explicitly accounts for the actuator dynamics. Specifically, a dual-mode Lyapunov-based EMPC (LEMPC) is designed with a combined process-actuator model. Conditions that guarantee the stability of the resulting closed-loop system under LEMPC and the regulatory layer are derived. Under the first mode of operation, the LEMPC may dictate a potentially time-varying operating policy while maintaining the closed-loop state trajectory in a bounded set. Under the second mode of the operation, the LEMPC computes control actions that force the closed-loop state to converge to a small region around the steady-state. An EMPC system that accounts for actuator dynamics is applied to a chemical process example to study the effect of the actuators on performance and integral input constraint satisfaction.

Chapter 2

Preliminaries

2.1 Notation

The Euclidean norm of a vector is denoted as $|\cdot|$. A continuous function $\alpha : [0, a) \to [0, \infty)$ belongs to class $\mathcal{K}$ if it is strictly increasing and $\alpha(0) = 0$. A function $V : R^n \to R_{\geq 0}$ is positive definite if $V(x) > 0$ for all $x \neq 0$ and $V(0) = 0$ at $x = 0$. The symbol Ω_r denotes a level set of a positive definite scalar function $V : R^n \to R_{\geq 0}$ ($\Omega_r := \{x \in R^n \mid V(x) \leq r\}$ where $r > 0$). The notation $S(\Delta)$ signifies the family of functions that are piecewise constant for time intervals of length Δ. Set subtraction is signified by the symbol "\" (i.e., $A \setminus B = \{x \in A \mid x \notin B\}$).

2.2 Class of Process Systems

The class of process systems considered is described by a system of nonlinear first-order ordinary differential equations of the form:

$$\dot{x}(t) = f(x(t), u_a(t), w(t)) \tag{2.1}$$

where $x \in R^{n_x}$ is the process state vector, $u_a \in R^{n_u}$ is the control actuator output vector, and $w \in R^{n_w}$ is the disturbance vector. Owing to the physical limitations of the control actuators, there are bounds on the control actuator outputs: $u_{a,i} \in U_{a,i} := \{u_{a,i} \in R \mid u_{a,i}^{\min} \leq u_{a,i} \leq u_{a,i}^{\max}\}$ for $i = 1, \ \ldots, \ n_u$ where $u_{a,i}^{\min}$ and $u_{a,i}^{\max}$ denote the minimum and maximum allowable values of the ith actuator output, respectively. The norm of the disturbance vector is assumed to be bounded in the set: $W := \{w \in R^{n_w} | \ |w| \leq \theta\}$ where $\theta > 0$. The vector function $f(\cdot, \cdot, \cdot)$ describing the process dynamics is assumed to be locally Lipschitz on $R^{n_x} \times R^{n_u} \times R^{n_w}$, and the origin of the unforced system is taken to be an equilibrium point of Eq. 2.1 ($f(0, 0, 0) = 0$). The state of the process system of Eq. 2.1 is assumed to be measured synchronously at sampling times $\Delta > 0$. The discrete sampling time sequence is denoted as $\{t_{k \geq 0}\}$ where $t_k := t_0 + k\Delta$, t_0 is the initial time, and $k = 0, \ 1, \ \ldots$.

2.3 Control Actuator Modeling

Typically, a feedback control system is designed to stabilize the origin of the nonlinear process system of Eq. 2.1. Within this paradigm, the controller computes control actions $u_m(t)$ and the underlying assumption is that the actuators can instantaneously or nearly instantaneously (i.e., in a negligible amount of time relative to the time constants of process dynamics of Eq. 2.1) implement the computed control action ($u_a(t) \approx u_m(t)$ for almost all times). However, the control actuators are dynamic systems and the assumption that $u_a(t) \approx u_m(t)$ may not necessarily be applicable depending on the dynamics of the actuators, thereby potentially leading to significant constraint violations. To this end, the dynamics of the ith control actuator, which may be operating in closed-loop under a linear controller or

in open-loop, are assumed to be modeled by the following linear system:

$$\begin{aligned} \begin{bmatrix} \dot{x}_{a,i}(t) \\ \dot{\zeta}_i(t) \end{bmatrix} &= A_i \begin{bmatrix} x_{a,i}(t) \\ \zeta_i(t) \end{bmatrix} + B_i u_{m,i}(t) \\ u_{a,i}(t) &= C_i x_{a,i}(t) \end{aligned} \tag{2.2}$$

where $x_{a,i} \in R^{n_{s,i}}$ is the state vector describing the dynamics of the ith actuator, $\zeta_i \in R^{n_{c,i}}$ is the state vector of the controller, $u_{m,i} \in R$ is the requested input value or set-point of the control loop around the ith actuator, $u_{a,i} \in R$ is the output of the ith actuator, and the matrices A_i, B_i, and C_i are real matrices of appropriate dimensions. For the case that the control actuator operates in open-loop or in closed-loop under a static controller, the model of Eq. 2.2 does not include any controller states. In this modeling framework, the actuator output is subject to constraints which leads to output constraints. The output constraints can be converted into linear state constraints, that is the state $x_{a,i}$ must satisfy:

$$x_{a,i} \in X_{a,i} := \{x_{a,i} \in R^{n_{s,i}} \mid u_{a,i}^{\min} \leq C_i x_{a,i} \leq u_{a,i}^{\max}\} \ . \tag{2.3}$$

The reachable set-points or requested actuator values are given by the set:

$$U_{m,i} := \left\{u_{m,i} \in R \mid u_{m,i}^{\min} \leq u_{m,i} \leq u_{m,i}^{\max}\right\} \tag{2.4}$$

where $u_{m,i}^{\min} = u_{a,i}^{\min}/K_{p,i}$, $u_{m,i}^{\max} = u_{a,i}^{\max}/K_{p,i}$, and $K_{p,i}$ is the steady-state gain between the requested input $u_{m,i}$ and the actuator output $u_{a,i}$. Continuous state or output feedback of the actuator state $x_{a,i}(t)$ or output $u_{a,i}(t)$ is assumed. Given that the system of Eq. 2.2 is linear, state estimation can be carried out using standard techniques. Although not explicitly needed for the theoretical developments below, the dynamics of the control actuators are assumed to be decoupled from one another and the eigenvalues of A_i are assumed to be strictly in the left-half of the complex plane ($Re\,(\lambda_j) < 0$ for all j where λ_j is an eigenvalue of A_i). These assumptions are made to study the most typical case in practice and to clarify

the fact that the input $u_m(t)$ is used to stabilize the process dynamics (i.e., $u_m(t)$ is not used to stabilize the actuator dynamics).

A model describing the evolution of all n_u control actuators is constructed from the individual models of Eq. 2.2. Define the following integers:

$$n_s := \sum_{i=1}^{n_u} n_{s,i},\ n_c := \sum_{i=1}^{n_u} n_{c,i} \tag{2.5}$$

and the following vectors: $x_a^T(t) := \left[x_{a,1}^T(t)\ \cdots\ x_{a,n_u}^T(t)\right]$ and $\zeta^T(t) := \left[\zeta_1^T(t)\ \cdots\ \zeta_{n_u}^T(t)\right]$. The dynamic model describing the evolution of all of the control actuators is

$$\begin{aligned} \begin{bmatrix} \dot{x}_a(t) \\ \dot{\zeta}(t) \end{bmatrix} &= A \begin{bmatrix} x_a(t) \\ \zeta(t) \end{bmatrix} + B u_m(t) \\ u_a(t) &= C x_a(t) \end{aligned} \tag{2.6}$$

where $x_a \in X_a := X_{a,1} \times \cdots \times X_{a,n_u} \subset R^{n_s}$, $\zeta \in R^{n_c}$, $u_m \in U_m := U_{m,1} \times \cdots \times U_{m,n_u}$, $A \in R^{(n_s+n_c)\times(n_s+n_c)}$, $B \in R^{(n_s+n_c)\times n_u}$, and $C \in R^{n_u \times n_s}$. The state constraint $x_a \in X_a$ is used to ensure that the output constraint is satisfied.

2.4 Combined Process-Actuator Model

From the process model of Eq. 2.1 and the control actuator layer model of Eq. 2.6, a combined dynamic model can be constructed to be used within an EMPC system. Denote the state vector of the combined process-actuator dynamic system as $z^T(t) := \left[x^T(t)\ x_a^T(t)\ \zeta^T(t)\right]$ and the resulting combined process-actuator system is given by:

$$\dot{z}(t) = \begin{bmatrix} f(x(t), C x_a(t), w(t)) \\ A \begin{bmatrix} x_a(t) \\ \zeta(t) \end{bmatrix} + B u_m(t) \end{bmatrix} =: g(z(t), u_m(t), w(t)) \tag{2.7}$$

where $z \in R^{n_z}$ with $n_z = n_x + n_s + n_c$, and $g : R^{n_z} \times R^{n_u} \times R^{n_w} \to R^{n_z}$ is a locally Lipschitz vector function of its arguments (by the assumption imposed on $f(\cdot, \cdot, \cdot)$). Owing to the constraints imposed on x_a, z is subject to the constraint $z \in Z$ where Z is the set where the state constraint on x_a is satisfied, and any other state constraints imposed on x and ζ are also satisfied. The combined process-actuator system is illustrated by the dotted box in Fig. 1.1.

For the combined process and actuator system, the existence of a stabilizing controller $h(z) \in U_m$ is assumed that renders the origin of the nominal closed-loop system $\dot{z} = g(z, h(z), 0)$ asymptotically stable. Applying an appropriate converse theorem [22, 23, 24], there exists a continuously differentiable, positive definite Lyapunov function, $V : R^{n_z} \to R_{\geq 0}$, for the closed-loop system of Eq. 2.7 under the controller $h(z)$ that satisfies:

$$\alpha_1(|z|) \leq V(z) \leq \alpha_2(|z|) \tag{2.8a}$$

$$\frac{\partial V(z)}{\partial z} g(z, h(z), 0) \leq -\alpha_3(|z|) \tag{2.8b}$$

$$\left| \frac{\partial V(z)}{\partial z} \right| \leq \alpha_4(|z|) \tag{2.8c}$$

for all $z \in D$ where D is an open neighborhood of the origin and the functions $\alpha_i(\cdot)$, $i = 1, 2, 3, 4$ are class $\mathcal{K}$ functions. Many nonlinear control laws have been developed for various classes of nonlinear systems that satisfy the aforementioned assumption (e.g., [25, 26, 27]).

An invariant set within D, usually taken to be a level set of V, will be used in the design of an EMPC system and is taken as an estimate of the region of attraction of $g(z, h(z), 0)$. Specifically, the level set of $V(\cdot)$, $\Omega_{\bar{\rho}} \subset D$, is defined which contains points in state-space where $\dot{V}(z) < 0$ when $z \neq 0$ and $\dot{V}(0) = 0$ while accounting for the input constraints. To account for the state constraints imposed on the state z, another level set Ω_ρ which satisfies $\Omega_\rho \subseteq Z$ and $\Omega_\rho \subseteq \Omega_{\bar{\rho}}$ is defined and is referred to as the stability region of the system of Eq. 2.7 under the controller $h(z)$ for the remainder.

Remark 1. A clarification on the stability region Ω_ρ is in order. First, when $\Omega_{\bar{\rho}} = Z$, the stability region Ω_ρ can be taken to be $\Omega_{\bar{\rho}}$ since this is a state-space region where $\dot{V}$ is negative definite and the state constraints are satisfied. However, consider two cases: $\Omega_{\bar{\rho}} \subset Z$ and $Z \subset \Omega_{\bar{\rho}}$. In the former case, the stability region Ω_ρ can be taken to be $\Omega_{\bar{\rho}}$ because the state constraints are satisfied for all points in $\Omega_{\bar{\rho}}$. While points outside of $\Omega_{\bar{\rho}}$ satisfy the state constraints, it may not be possible to stabilize the closed-loop system for any states starting in $Z \setminus \Omega_{\bar{\rho}}$ given that the time-derivative of the Lyapunov function is not guaranteed to be negative. For the latter case, Ω_ρ needs to be taken to be a subset of Z. Any point starting in Z does satisfy the state constraint and is such that $\dot{V}$ is negative definite. However, the closed-loop state trajectory that the system evolves along under the controller $h(z)$ is not guaranteed to be maintained in Z, i.e., Z may not necessarily be forward invariant for the closed-loop system. The state trajectory may come out of Z, but stay in $\Omega_{\bar{\rho}}$, before it asymptotically converges to the origin.

Remark 2. When the response of the control actuators is sufficiently fast such that the system of Eq. 2.7 exhibits two-time-scale dynamics and A has eigenvalues with negative real parts, the assumption of the existence of a stabilizing controller can be made with respect to the process dynamics of Eq. 2.1, and the design of the EMPC may proceed with neglecting the control actuator dynamics. In this work, the more general case where the combined system of Eq. 2.7 does not necessarily exhibit two-time-scale dynamics is considered. A motivating example is given in the subsequent section to better illustrate the complications arising when a sufficient time-scale separation between the process dynamics and the actuator dynamics is not present. Moreover, when the process-actuator dynamics exhibit two-time-scale dynamics, designing a controller $h(z)$ which includes both the fast and slow system states may lead to an ill-conditioned controller (see, for example, [28] for some results on two-time-scale systems within the context of EMPC).

2.5 Economic Model Predictive Control

A scalar function $l : R^{n_x} \times R^{n_u} \rightarrow R$ that captures the real-time process economics is used as the stage cost in EMPC. As previously discussed, the control actuator dynamics are typically neglected when designing and studying the stability and performance properties of EMPC with $u_a(t) = u_m(t)$. In this context, EMPC is characterized by the following dynamic optimization problem:

$$\underset{u_m \in S(\Delta)}{\text{minimize}} \quad \int_{t_k}^{t_k+N\Delta} l(\tilde{x}(\tau), u_m(\tau))\, d\tau \tag{2.9a}$$

$$\text{subject to} \quad \dot{\tilde{x}}(t) = f(\tilde{x}(t), u_m(t), 0) \tag{2.9b}$$

$$\tilde{x}(t_k) = x(t_k) \tag{2.9c}$$

$$u_m(t) \in U_m \tag{2.9d}$$

where the decision variable of the optimization problem is the piecewise constant input trajectory $u_m(t)$ that is defined over the prediction horizon $t \in [t_k, t_k + N\Delta)$. The EMPC uses the nominal process model (Eq. 2.9b) initialized with a state feedback measurement at the current sampling time t_k (Eq. 2.9c) to predict the evolution of the process over the prediction horizon. The predicted state trajectory is denoted as $\tilde{x}(t)$. The input constraints (Eq. 2.9d) are included as a constraint in the optimization problem to ensure that the EMPC computes an admissible control action. The EMPC is typically implemented in a receding horizon fashion: at a sampling period t_k, a state measurement is received, the optimal control problem defined by Eq. 2.9 is solved for the optimal input trajectory denoted as $u_m^*(t|t_k)$ where $t \in [t_k, t_k + N\Delta)$, and the control action defined for the first sampling period of the prediction horizon, which is denoted as $u_m^*(t_k|t_k)$, is sent to the control actuator layer to be implemented over the sampling period. At the next sampling period t_{k+1}, the procedure is repeated. In general, EMPC, as defined by the problem of Eq. 2.9, is not stabilizing

and thus, additional constraints are added to the problem of Eq. 2.9 to ensure closed-loop stability. In this work, stability constraints will be designed on the basis of the explicit feedback controller $h(z)$.

Chapter 3

EMPC Accounting for the Control Actuator Dynamics

In this section, the design of an Lyapunov-based EMPC (LEMPC) scheme that accounts for the control actuator layer and a stability analysis of the closed-loop process-actuator system of Eq. 2.7 under the LEMPC is completed. To better illustrate the complications arising from the actuator layer, a motivating example is given in the next subsection.

3.1 Motivating Example

Consider the following scalar nonlinear system:

$$\dot{x} = x^2 + u_a \tag{3.1}$$

where $u_a \in [-10, 10]$. The (open-loop) dynamics of the control actuator are assumed to be described by the following first-order transfer function (in the Laplace domain):

$$G_p(s) = \frac{K_p}{\tau_P s + 1} \tag{3.2}$$

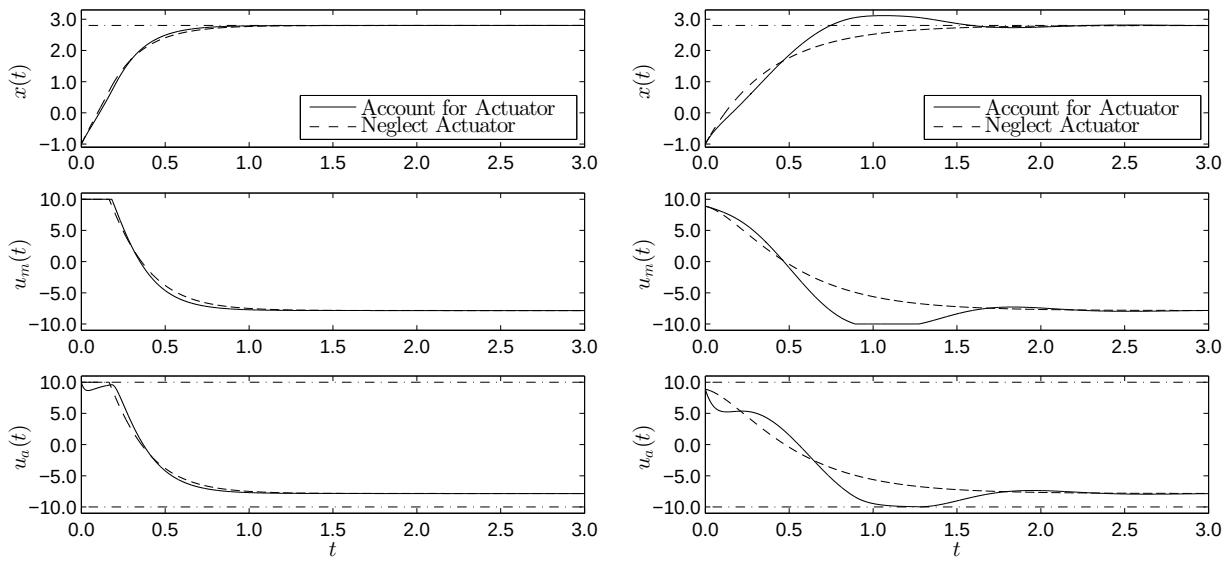

(a) (b)

Figure 3.1: The transient response of the closed-loop system resulting from the process described by Eq. 3.1 and a first-order control actuator controlled by a PI controller with controller parameters: (a) $K_c = 5.0$ and $K = 5.0$ and (b) $K_c = 1.0$ and $K = 2.6$ (which is denoted as "Account for Actuator"). For comparison purposes, the case when $u_a(t) = u_m(t)$ is also given and is denoted as "Neglect Actuator".

where K_p is the steady-state process gain and τ_P is the time constant. For this example, let $K_p = 1.0$ and $\tau_P = 0.1$. The control actuator is regulated by a PI controller which has the following transfer function:

$$G_c(s) = K_c \left(1 + \frac{1}{\tau_I s}\right) \tag{3.3}$$

where K_c is the controller gain and τ_I is the integral/reset time. Let $K_c = 5.0$ and $\tau_I = 0.1$ which has been tuned so that the closed-loop transfer function relating the desired input u_m to the actuator output u_a is over-damped. A feedback controller is designed via feedback linearization techniques to stabilize an operating steady-state of the system of Eq. 3.1 by neglecting the control actuator layer and is given by the following explicit control law:

$$u_m(t) = -x^2 + K\left(x_{sp} - x\right) \tag{3.4}$$

where x_{sp} is the desired operating steady-state and K is a tuning parameter of the controller.

In this case, let $K = 5.0$ and $x_{sp} = 2.8$. An example transient response of the resulting closed-loop system is given in Fig. 3.1a along with the case that $u_a(t) = u_m(t)$. From Fig. 3.1a, the transient response of the closed-loop system including the actuator dynamics nearly overlaps the response of the case when $u_a(t) = u_m(t)$. For this case, the upper bound on K for closed-loop stability is large given that the closed-loop actuator tracks $u_m(t)$ sufficiently fast (i.e., K may be increased to increase the speed of the response of $x(t)$). In addition, when $u_a(t) = u_m(t)$, there is no upper bound on K.

On the other hand, consider a different case where $K_c = 1.0$ (the remaining parameters are the same as the previous case). With this PI controller gain, the closed-loop system is unstable because the closed-loop actuator does not respond sufficiently fast. To make the closed-loop system stable, one could decrease the feedback linearizing controller gain (effectively slowing the rate of change of $u_m(t)$). A closed-loop simulation with $K = 2.8$ and $K_c = 1.0$ is shown in Fig. 3.1b. The closed-loop state trajectory $x(t)$ is driven to the desired set-point which demonstrates that with $K_c = 1.0$ there is an upper bound on the feedback linearizing controller gain, K, for closed-loop stability. However, compared to the case where $u_m(t) = u_a(t)$ (denoted as "Neglect Actuator" in Fig. 3.1b), the transient response is much different. For example, overshoot is observed in the state trajectory $x(t)$ where the closed-loop actuator under the PI controller dynamics is simulated, while no overshoot is observed for the case where the actuator layer is neglected in the simulation. The discrepancy noticed in the closed-loop state trajectories of Fig. 3.1b is an important consideration in the context of EMPC as consistently transient operation may be realized under EMPC. If one does not account for the actuator layer and the response of the process system is sufficiently different from that predicted by the model, closed-loop performance under EMPC may be significantly affected.

3.2 Lyapunov-based EMPC Formulation and Implementation

An EMPC is designed via the Lyapunov-based techniques proposed in [20] which takes advantage of the stability properties of an explicit stabilizing controller. To account for the actuator dynamics, the combined process-actuator model of Eq. 2.7 and the controller $h(z)$ are used in the formulation. With abuse of notation, $l(z)$ will be used to denote the economic stage cost $l(x, u_a)$. However, one may also consider more general stage cost functions which may include the regulatory controller states ζ and/or the requested control actions u_m in the economic stage cost because the stability analysis of LEMPC does not rely on the objective function value to have certain properties to prove closed-loop stability. The resulting Lyapunov-based EMPC (LEMPC) is formulated as follows:

$$\min_{u_m \in S(\Delta)} \quad \int_{t_k}^{t_k+N\Delta} l(\tilde{z}(\tau))\, d\tau \tag{3.5a}$$

$$\text{subject to} \quad \dot{\tilde{z}}(t) = g(\tilde{z}(t), u_m(t), 0) \tag{3.5b}$$

$$\tilde{z}(t_k) = z(t_k) \tag{3.5c}$$

$$u_m(t) \in U_m, \ \forall\ t \in [t_k, t_k + N\Delta) \tag{3.5d}$$

$$V(\tilde{z}(t)) \leq \rho_e, \ \forall\ t \in [t_k, t_k + N\Delta),$$

$$\text{if } t_k < t' \text{ and } V(z(t_k)) \leq \rho_e \tag{3.5e}$$

$$\frac{\partial V(z(t_k))}{\partial z} g(z(t_k), u_m(t_k), 0)$$

$$\leq \frac{\partial V(z(t_k))}{\partial z} g(z(t_k), h(z(t_k)), 0),$$

$$\text{if } t_k \geq t' \text{ or } V(z(t_k)) > \rho_e \tag{3.5f}$$

where the decision variable is the requested piecewise constant input trajectory $u_m(t)$ which is defined over the prediction horizon $t \in [t_k, t_k + N\Delta)$ and $\tilde{z}(t)$ denotes the predicted state trajectory.

The LEMPC of Eq. 3.5 is a dual mode controller and t' denotes a switching time between modes. Under Mode 1 operation ($t_k < t'$), the LEMPC operates the process system in an economically optimal, but possibly transient, manner while maintaining the closed-loop state in Ω_ρ. To guarantee that the closed-loop state, which can be affected by unknown bounded disturbances, will be maintained in Ω_ρ, two Lyapunov-based constraints of Eq. 3.5e-3.5f are used. If the state of the system is in $\Omega_{\rho_e} \subset \Omega_\rho$, then the constraint of Eq. 3.5e is active and defines Mode 1 operation of the LEMPC. Eq. 3.5e constrains the predicted state trajectory to be contained in Ω_{ρ_e} over the prediction horizon. The region Ω_{ρ_e} is designed to be such that any state starting in Ω_{ρ_e} will be maintained in Ω_ρ over the sampling period in the presence of bounded disturbances, so that the state at the next sampling period will be in Ω_ρ. If the current state $z(t_k) \notin \Omega_{\rho_e}$, the constraint of Eq. 3.5f, which defines Mode 2 operation, is active. This contractive constraint enforces that the time-derivative of the Lyapunov function under the control action implemented at the first sampling period of the prediction horizon be less than that under the control action computed by the controller $h(z)$. This will guarantee that any state starting in $\Omega_\rho \setminus \Omega_{\rho_e}$ will converge to Ω_{ρ_e} in finite time. Under Mode 2 operation ($t_k \geq t'$), the contractive constraint of Eq. 3.5f is always active which enforces that the closed-loop state converges to a small compact set containing the origin in its interior. The LEMPC of Eq. 3.5 is implemented in a receding horizon fashion.

Remark 3. It is important to point out that the constraints on the control actuator outputs (i.e., the state constraints) are guaranteed to be satisfied for the closed-loop system under LEMPC with any initial state $z(t_0) \in \Omega_\rho$ because the closed-loop state under the LEMPC of Eq. 3.5 is guaranteed to be maintained in Ω_ρ. Within Ω_ρ, the state constraints are satisfied by design of the region Ω_ρ.

3.3 Stability Analysis

By design of the controller $h(z)$, the stability region Ω_ρ, and the Lyapunov-based constraints imposed in the LEMPC (Eqs. 3.5e-3.5f), the resulting LEMPC scheme has the same closed-loop stability and robustness properties (with respect to the closed-loop system of Eq. 2.7) as that described in [20]. For completeness of presentation, the stability properties are summarized below (the proofs of Propositions 1-2 can be found in [29] and the proof of Theorem 1 in [20]). The results utilize the following properties which follow from the fact that $g(\cdot,\cdot,\cdot)$ is a locally Lipschitz vector function in its arguments, the Lyapunov function $V(\cdot)$ is continuously differentiable, and the state vector z, the input vector u_m, and the disturbance vector w are all bounded in a compact set. First, there exists an $M > 0$ such that:

$$|g(z, u_m, w)| \leq M \tag{3.6}$$

for all $z \in \Omega_\rho$, $u_m \in U_m$, and $w \in W$. Second, there exist positive constants L_z, L_w, L'_z, and L'_w such that:

$$|g(z_1, u_m, w) - g(z_2, u_m, 0)| \leq L_z|z_1 - z_2| + L_w|w| \tag{3.7}$$

$$\left|\frac{\partial V(z_1)}{\partial z} g(z_1, u_m, w) - \frac{\partial V(z_2)}{\partial z} g(z_2, u_m, 0)\right| \leq L'_z|z_1 - z_2| + L'_w|w| \tag{3.8}$$

for all z_1, $z_2 \in \Omega_\rho$, $u_m \in U_m$ and $w \in W$.

The following proposition bounds the difference between Lyapunov function values for any two points in Ω_ρ.

Proposition 1 (c.f. [29])**.** *The difference between Lyapunov function value for any two points in Ω_ρ is bounded by a quadratic function $f_V(\cdot)$:*

$$V(z_1) - V(z_2) \leq f_V(|z_1 - z_2|) \tag{3.9}$$

for all $z_1,\ z_2 \in \Omega_\rho$ *where*

$$f_V(s) := \alpha_4(\alpha_1^{-1}(\rho))s + \beta s^2 \tag{3.10}$$

for some $\beta > 0$.

The difference between the nominal state trajectory of Eq. 2.7 ($w(t) \equiv 0$) and the state trajectory in the presence of disturbances can be bounded when the state trajectories are maintained in Ω_ρ.

Proposition 2 (c.f. [29])**.** *The difference between the state trajectory of Eq. 2.7 where* $w(t) \not\equiv 0$ *and the nominal state trajectory of Eq. 2.7 (*$w(t) \equiv 0$*) can be bounded by a class* $\mathcal{K}$ *function* $f_w(\cdot)$*:*

$$|z(t) - \hat{z}(t)| \leq f_w(t - t_0) \tag{3.11}$$

when $z(\tau),\ \hat{z}(\tau) \in \Omega_\rho$ *for all* $\tau \in [t_0, t]$ *where* $z(t)$ *denotes the state of the system of Eq. 2.7 with* $w(t) \not\equiv 0$ *and* $\hat{z}(t)$ *denotes the state of the nominal system of Eq. 2.7 and*

$$f_w(s) := \frac{L_w \theta}{L_x}\left(e^{L_x s} - 1\right)\ . \tag{3.12}$$

The following theorem states the stability properties of the closed-loop system of Eq. 2.7 under the LEMPC of Eq. 3.5. For any state $z(t_0) \in \Omega_\rho$, sufficiently small sampling period and bound on disturbance, and ρ_e properly chosen, the closed-loop state trajectory will be maintained in Ω_ρ. If the switching time t' is finite (i.e., the LEMPC switches to Mode 2 operation only), the closed-loop state converges to and remains bounded in a small invariant set containing the origin in its interior.

Theorem 1 (c.f. [20])**.** *Consider the closed-loop system of Eq. 2.7 under the LEMPC of Eq. 3.5 based on a controller* $h(z)$ *that satisfies the conditions of Eq. 2.8. Let* $\epsilon_w > 0$, $\Delta > 0$, $\rho > \rho_e > 0$ *and* $\rho > \rho_s > 0$ *satisfy*

$$\rho_e \leq \rho - f_V(f_w(\Delta)) \tag{3.13}$$

and

$$-\alpha_3(\alpha_2^{-1}(\rho_s)) + L_z' M\Delta + L_w'\theta \leq -\epsilon_w/\Delta \ . \tag{3.14}$$

If $z(t_0) \in \Omega_\rho$, $\rho_s \leq \rho_e$, $\rho_{\min} \leq \rho$ *and* $N \geq 1$ *where*

$$\rho_{\min} = \max\{V(z(t+\Delta)) \mid V(z(t)) \leq \rho_s\} \tag{3.15}$$

then the state $z(t)$ *of the closed-loop system is always bounded in* Ω_ρ. *Furthermore, if the switching time is finite* ($t' < \infty$) , *then the closed-loop state* $z(t)$ *is ultimately bounded in* $\Omega_{\rho_{\min}}$.

Chapter 4

Application to a Chemical Process Example

A benchmark chemical reactor example from [30] is considered in this case study. Specifically, consider a continuously stirred tank reactor (CSTR) where ethylene (C_2H_4) is oxidized to ethylene oxide (C_2H_4O). The CSTR is equipped with a cooling jacket to remove heat generated from the exothermic reactions occurring in the CSTR. In addition to the catalytic oxidation reaction that converts ethylene to ethylene oxide, two combustion reactions that convert ethylene oxide and ethylene to carbon dioxide and water occur in the CSTR. The reaction equations are as follows:

$$C_2H_4 + \frac{1}{2}O_2 \xrightarrow{r_1} C_2H_4O \tag{R1}$$

$$C_2H_4 + 3O_2 \xrightarrow{r_2} 2CO_2 + 2H_2O \tag{R2}$$

$$C_2H_4O + \frac{5}{2}O_2 \xrightarrow{r_3} 2CO_2 + 2H_2O \tag{R3}$$

Table 4.1: Dimensionless process model parameters of the ethylene oxidation CSTR. The parameters are taken from [30].

Parameter	Value	Parameter	Value
A_1	92.80	B_4	7.02
A_2	12.66	γ_1	-8.13
A_3	2412.71	γ_2	-7.12
B_1	7.32	γ_3	-11.07
B_2	10.39	T_c	1.0
B_3	2170.57		

The reaction rates r_1, r_2, and r_3 of reactions R1-R3, respectively, are given by the following rate laws [31]:

$$r_1 = k_1 \exp\left(\frac{-E_1}{RT}\right) P_E^{0.5} \tag{4.1a}$$

$$r_2 = k_2 \exp\left(\frac{-E_2}{RT}\right) P_E^{0.25} \tag{4.1b}$$

$$r_3 = k_3 \exp\left(\frac{-E_3}{RT}\right) P_{EO}^{0.5} \tag{4.1c}$$

where k_1, k_2, and k_3 are pre-exponential factors, E_1, E_2, and E_3 are activation energies for each reaction, R is the gas constant, and T is the absolute temperature. The reaction rates depend on the partial pressures of ethylene (P_E) and of ethylene oxide (P_{EO}). The gaseous mixture in the CSTR is assumed to be an ideal gas, and thus, the partial pressures can be written in terms of the molar concentrations of ethylene and ethylene oxide which are denoted as C_E and C_{EO}, respectively.

A system of four differential equations relating the state variables for the chemical process (reactor gas density (ρ_R), ethylene concentration (C_E), ethylene oxide concentration (C_{EO}), and absolute temperature T within the reactor) can be derived from mass and energy balances by employing standard modeling assumptions (a detailed description of the modeling can be found in [30]). To simplify the presentation, a dimensionless variable form of the reactor model will be used with the state variables ρ_R, C_E, C_{EO}, and T corresponding to

the dimensionless state variables x_1, x_2, x_3, and x_4, respectively. The system of ordinary differential equations that describes the evolution of the CSTR is given by:

$$\frac{dx_1}{dt} = u_1(1 - x_1x_4) \tag{4.2a}$$

$$\frac{dx_2}{dt} = u_1(u_2 - x_2x_4) - A_1 \exp(\gamma_1/x_4)(x_2x_4)^{1/2} - A_2 \exp(\gamma_2/x_4)(x_2x_4)^{1/4} \tag{4.2b}$$

$$\frac{dx_3}{dt} = -u_1x_3x_4 + A_1 \exp(\gamma_1/x_4)(x_2x_4)^{1/2} - A_3 \exp(\gamma_3/x_4)(x_3x_4)^{1/2} \tag{4.2c}$$

$$\begin{aligned}\frac{dx_4}{dt} = {} & \frac{u_1}{x_1}(1 - x_4) + \frac{B_1}{x_1} \exp(\gamma_1/x_4)(x_2x_4)^{1/2} + \frac{B_2}{x_1} \exp(\gamma_2/x_4)(x_2x_4)^{1/4} \\ & + \frac{B_3}{x_1} \exp(\gamma_3/x_4)(x_3x_4)^{1/2} - \frac{B_4}{x_1}(x_4 - T_c)\end{aligned} \tag{4.2d}$$

where A_j ($j = 1,\ 2,\ 3$), B_k ($k = 1,\ 2,\ 3,\ 4$), γ_l ($l = 1,\ 2,\ 3$), and T_c are process parameters with values given in Table 4.1 and t denotes the dimensionless time. The manipulated inputs to the reactor are considered to be the volumetric flow rate of the inlet stream (u_1) and the concentration of ethylene in the inlet stream (u_2). The output of actuators for the manipulated inputs u_1 and u_2 is assumed to be the inlet volumetric flow rate and the inlet concentration of ethylene, respectively. The actuator outputs are bounded within the following sets:

$$u_{a,1} \in [0.0704,\ 0.7042]$$

$$u_{a,2} \in [0.2465,\ 2.4648]$$

The control objective of the CSTR is to feed the ethylene to the reactor in a manner that maximizes the average yield of ethylene oxide. The average yield of ethylene oxide, which quantifies the amount of ethylene oxide produced compared to the amount of ethylene fed

to the reactor, is given by:

$$Y(t_f) = \frac{\int_{t_0}^{t_f} u_1(\tau)x_3(\tau)x_4(\tau)\ d\tau}{\int_{t_0}^{t_f} u_1(\tau)u_2(\tau)\ d\tau} \tag{4.3}$$

where t_0 is the initial time and t_f is the final time. Owing to practical considerations, the time-averaged molar flow rate of ethylene that can be fed to the reactor is limited to:

$$\frac{1}{t_f - t_0}\int_{t_0}^{t_f} u_1(\tau)u_2(\tau)\ d\tau = 0.175\ . \tag{4.4}$$

Because the integral input constraint of Eq. 4.4 fixes the value of the denominator in Eq. 4.3, the stage cost function used in the EMPC problem to achieve the desired objective is:

$$l(x,u) = -u_1x_3x_4\ . \tag{4.5}$$

The control actuators for the manipulated inputs u_1 and u_2 are modeled as identical first-order linear systems with transfer function (in the Laplace domain):

$$G_p(s) = \frac{K_p}{\tau_P s + 1} \tag{4.6}$$

where the steady-state gain of the actuators is $K_p = 1.0$ and the time-constant of the actuators is $\tau_p = 0.0225$. Each control actuator output is controlled by a PI controller which receives its set-point from the EMPC in the supervisory layer (c.f. Fig. 1.1). The transfer function describing the PI controllers (the same tuning parameters were used in both PI controllers) is:

$$G_c(s) = K_c\left(1 + \frac{1}{\tau_I s}\right) \tag{4.7}$$

where the PI controllers in the simulations below have been tuned to give over-damped responses. Thus, the closed-loop dynamics of a control actuator under a PI controller form

a second-order linear system and the dynamic equations modeling the closed-loop behavior have two states: $u_{a,i}$, which is the ith actuator output, and ζ_i, which is the ith PI controller state ($i = 1,\ 2$). The input to the closed-loop system consisting of the actuator under the PI controller is the set-point $u_{m,i}$ of the control loop and is computed by the EMPC. Under the modeling framework of Eq. 2.7, the state of the combined process-actuator model is $z^T = [x_1\ x_2\ x_3\ x_4\ u_{a,1}\ u_{a,2}\ \zeta_1\ \zeta_2]$ and the input is $u_m^T = [u_{m,1}\ u_{m,2}]$.

In this case study, the difference between accounting for the control actuator layer in EMPC and neglecting the actuator layer will be examined. Two EMPC systems are considered. Before the EMPC is designed, it is important to point out that the system has an open-loop asymptotically stable steady-state that satisfies the integral input constraint of Eq. 4.4 with $x_s^T = [0.998\ \ 0.424\ \ 0.032\ \ 1.002]$ which corresponds to the steady-state input $u_s^T = [0.35\ \ 0.5]$. Since closed-loop stability under EMPC is not an issue for the region of operation considered for the system of Eq. 4.2, an explicit characterization of the Lyapunov-based constraints of Eqs. 3.5e-3.5f will not be needed. However, given that the steady-state is open-loop asymptotically stable, there exists a control Lyapunov function that could be used to design a Lyapunov-based controller that satisfies Eq. 2.8b. With the Lyapunov function and Lyapunov-based controller, the Lyapunov-based constraints of Eqs. 3.5e-3.5f could be designed.

To satisfy the integral input constraint of Eq. 4.4 over the entire length of operation given the EMPC is formulated with a finite-time prediction horizon, the constraint is imposed over successive operating windows, that is the constraint must be satisfied over each operating interval of length t_p. The EMPC systems considered are implemented with a shrinking horizon that covers the entire operating window t_p at the beginning of the window and is decremented by one at each sampling period. Specifically, at the beginning of the operating window where $t_k = t_0 + jt_p$ for some $j = 0,\ 1,\ \ldots$ (j denotes the jth operating window), the prediction horizon is initialized as $N_k = t_p/\Delta$ (assuming that t_p is a multiple of the sampling period). At each subsequent sampling period, the prediction horizon decreases by

one ($N_k = N_{k-1} - 1$) until the beginning of the next operating window where the prediction horizon is reinitialized to t_p/Δ.

The formulation of the EMPC that does not account for the actuator layer is given by:

$$\min_{u_m \in S(\Delta)} -\int_{t_k}^{t_k+N_k\Delta} u_{m,1}(\tau)\tilde{x}_3(\tau)\tilde{x}_4(\tau)\ d\tau \tag{4.8a}$$

$$\text{s.t.} \quad \dot{\tilde{x}}(t) = f(\tilde{x}(t), u_m(t)) \tag{4.8b}$$

$$\tilde{x}(t_k) = x(t_k) \tag{4.8c}$$

$$u_{m,1}(t) \in [0.0704,\ 0.7042] \tag{4.8d}$$

$$u_{m,2}(t) \in [0.2465,\ 2.4648] \tag{4.8e}$$

$$\frac{1}{t_p}\int_{t_k}^{t_k+N_k\Delta} u_{m,1}(\tau)u_{m,2}(\tau)\ d\tau$$

$$= 0.175 - \frac{1}{t_p}\int_{t_0+jt_p}^{t_k} u^*_{m,1}(\tau)u^*_{m,2}(\tau)\ d\tau \tag{4.8f}$$

where the constraints of Eq. 4.8d-4.8e are enforced for all $t \in [t_k, t_k+N_k\Delta)$ and the integral of the right-hand side of Eq. 4.8f accounts for the amount of material used since the beginning of the operating window. The EMPC of Eq. 4.8 will be referred to as EMPC-1 for the remainder. The formulation of the EMPC that accounts for the actuator dynamics, which will be referred to as EMPC-2 for the remainder, is given by:

$$\min_{u_m \in S(\Delta)} -\int_{t_k}^{t_k+N_k\Delta} \tilde{z}_5(\tau)\tilde{z}_3(\tau)\tilde{z}_4(\tau)\ d\tau \tag{4.9a}$$

$$\text{s.t.} \quad \dot{\tilde{z}}(t) = g(\tilde{z}(t), u_m(t)) \tag{4.9b}$$

$$\tilde{z}(t_k) = z(t_k) \tag{4.9c}$$

$$\tilde{z}_5(t) \in [0.0704,\ 0.7042] \tag{4.9d}$$

$$\tilde{z}_6(t) \in [0.2465,\ 2.4648] \tag{4.9e}$$

$$u_{m,1}(t) \in [0.0704,\ 0.7042] \tag{4.9f}$$

$$u_{m,2}(t) \in [0.2465,\ 2.4648] \tag{4.9g}$$

$$\frac{1}{t_p}\int_{t_k}^{t_k+N_k\Delta} \tilde{z}_5(\tau)\tilde{z}_6(\tau)\ d\tau$$

$$= 0.175 - \frac{1}{t_p}\int_{t_0+jt_p}^{t_k} z_5^*(\tau)z_6^*(\tau)\ d\tau \tag{4.9h}$$

where the constraints of Eq. 4.9d-4.9g are enforced for all $t \in [t_k, t_k+N_k\Delta)$ and the integral of the right-hand side of Eq. 4.9h accounts for the actual amount of material fed to the reactor (i.e., the actual actuator output). A notable difference between EMPC-1 and EMPC-2 is in the enforcement of the integral constraint. Because EMPC-1 neglects the actuator dynamics, while EMPC-2 includes them, in EMPC-1, the integral input constraint is enforced on the basis of the requested input, while EMPC-2 enforces the constraint to be satisfied on that which is actually being fed to the reactor.

The sampling period used in the implementation of EMPC-1 and EMPC-2 is $\Delta = 9.36$, and the operating window for which the integral input constraints are enforced is $t_p = 46.8$. All numerical integrations were performed using the explicit Euler method with a step size of $h = 0.0001$ used to integrate forward the model within each EMPC optimization problem and a step size of $h_i = 0.00001$ to simulate the closed-loop dynamics of the reactor and actuators. In the closed-loop simulations below, the reactor was initialized at $z^T(0) = [0.997\ \ 1.264\ \ 0.209\ \ 1.004\ \ 0\ \ 0\ \ 0\ \ 0]$. The state constraints on the components of u_a in Eqs. 4.9d-4.9e are enforced at every integration step h. To solve the optimization problems, the open-source interior point solver, Ipopt [32] was employed.

Three different PI tunings for the actuator controllers were considered. The tunings were chosen by finding values of K_c with $\tau_I = \tau_P = 0.0225$ such that the step response to a

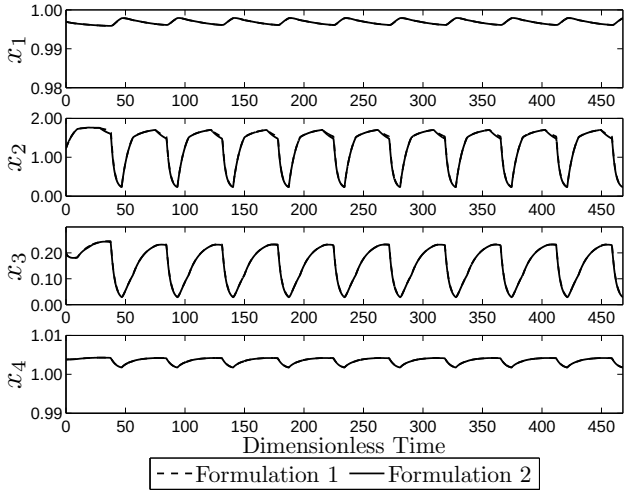

Figure 4.1: The closed-loop state trajectories of the CSTR under EMPC-1 (dashed line) and under EMPC-2 (solid line) with $K_c = 0.09$ (the trajectories are overlapping).

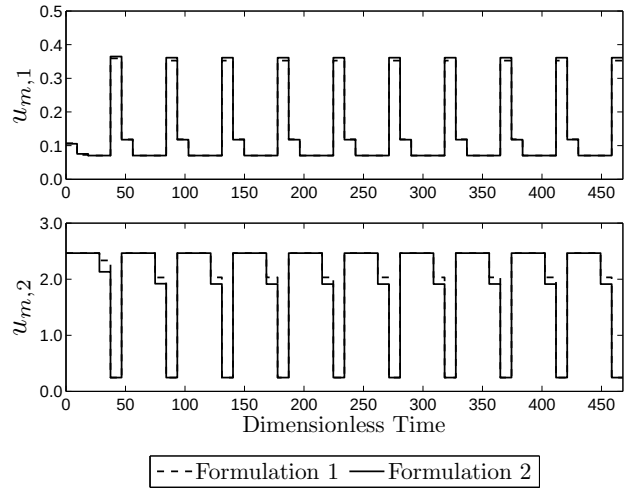

Figure 4.2: The requested input trajectory ($u_m(t)$) computed by EMPC-1 (dashed line) and by EMPC-2 (solid line) corresponding to the case $K_c = 0.09$ (the trajectories are nearly overlapping).

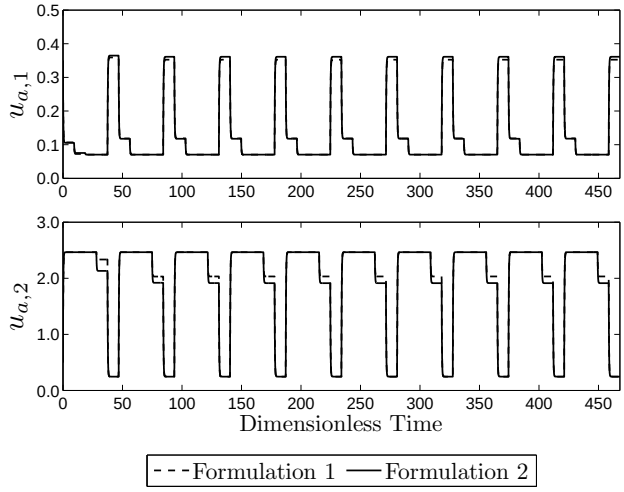

Figure 4.3: The control actuator output trajectory ($u_a(t)$) for the closed-loop CSTR under EMPC-1 (dashed line) and EMPC-2 (solid line) with $K_c = 0.09$ (the trajectories are nearly overlapping).

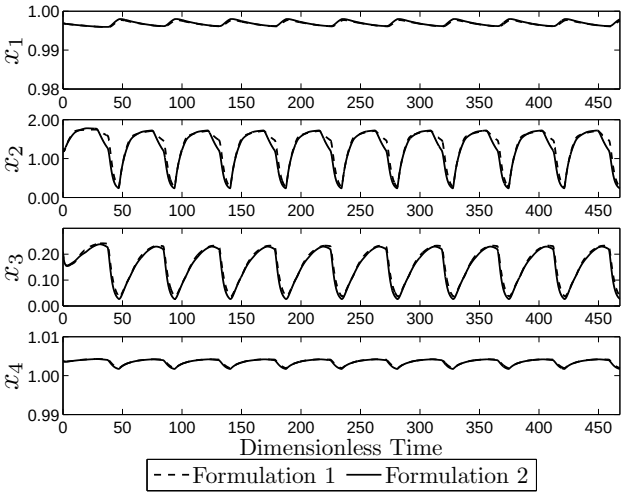

Figure 4.4: The closed-loop state trajectories of the CSTR under EMPC-1 (dashed line) and under EMPC-2 (solid line) with $K_c = 0.02$ (the trajectories are nearly overlapping).

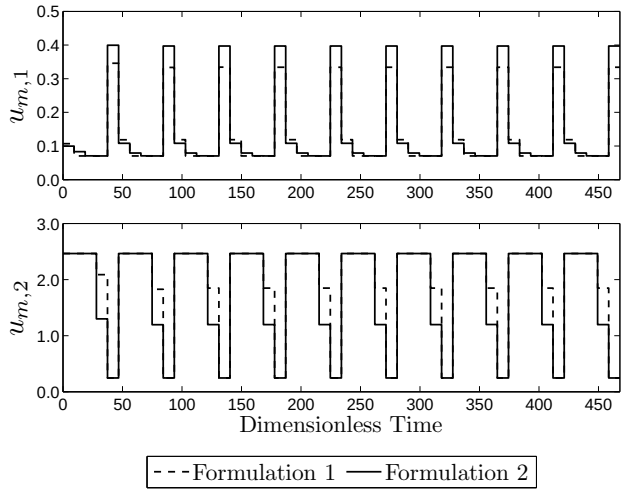

Figure 4.5: The requested input trajectory ($u_m(t)$) computed by EMPC-1 (dashed line) and by EMPC-2 (solid line) corresponding to the case $K_c = 0.02$.

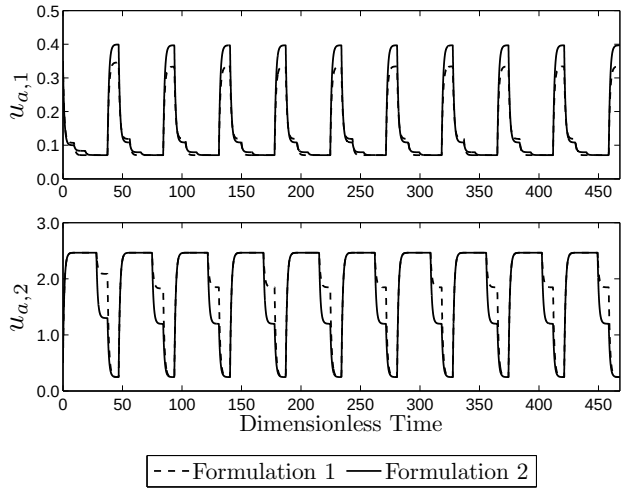

Figure 4.6: The control actuator output trajectory ($u_a(t)$) for the closed-loop CSTR under EMPC-1 (dashed line) and EMPC-2 (solid line) with $K_c = 0.02$.

Table 4.2: The average yield of ethylene oxide for the CSTR under EMPC-1 and under EMPC-2 over ten operating periods. The columns denoted as "Min. Con." and "Max. Con." correspond to the minimum and maximum average ethylene molar flow rate fed to the CSTR over an operating period.

	EMPC-1			EMPC-2		
Case	Yield	Min. Con.	Max. Con.	Yield	Min. Con.	Max. Con.
1	9.66%	0.1766	0.1770	9.60%	0.1750	0.1750
2	9.79%	0.1811	0.1826	9.53%	0.1750	0.1750
3	9.90%	0.1850	0.1858	9.41%	0.1750	0.1750

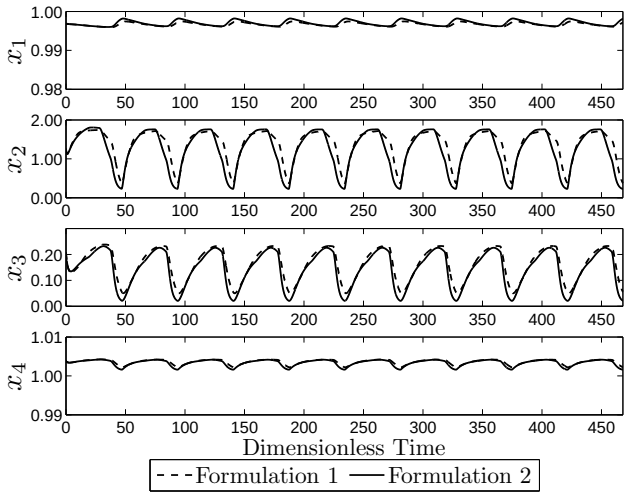

Figure 4.7: The closed-loop state trajectories of the CSTR under EMPC-1 (dashed line) and under EMPC-2 (solid line) $K_c = 0.01$.

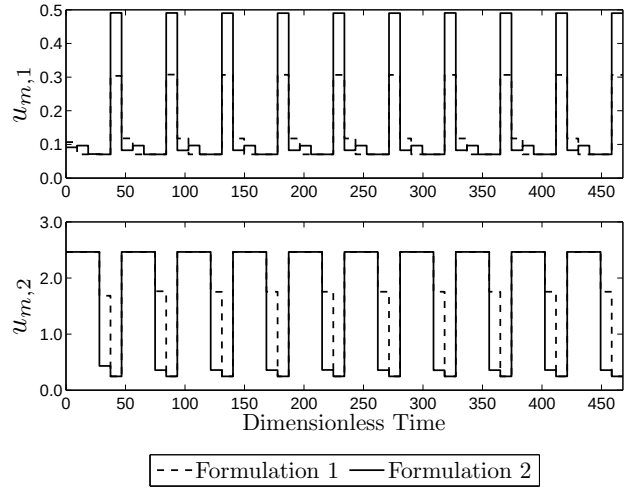

Figure 4.8: The requested input trajectory ($u_m(t)$) computed by EMPC-1 (dashed line) and by EMPC-2 (solid line) corresponding to the case $K_c = 0.01$.

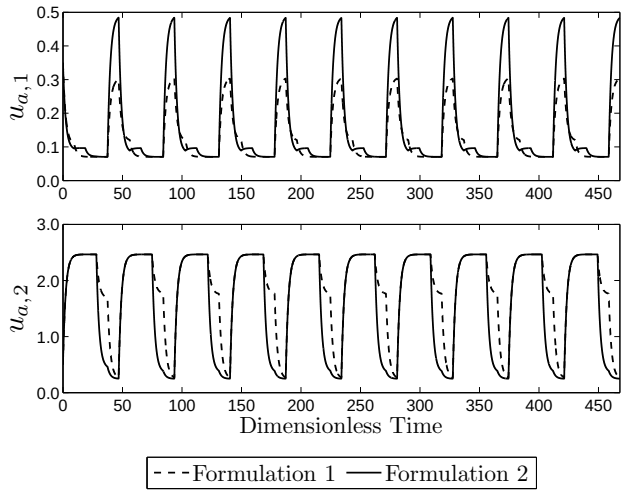

Figure 4.9: The control actuator output trajectory ($u_a(t)$) for the closed-loop CSTR under EMPC-1 (dashed line) and EMPC-2 (solid line) with $K_c = 0.01$.

change in set-point u_m would reach 98% of its final value in about 10%, 50%, and 100% of the sampling period $\Delta = 9.36$ without overshooting. The three tuning cases are referred to as Case 1, 2, and 3 for the remainder, and the proportional gains used were $K_c = 0.09$, $K_c = 0.02$, and $K_c = 0.01$, respectively, for the three cases.

Several closed-loop simulations under both EMPC-1 and EMPC-2 for the different tuning settings of the PI controllers were carried out over ten operating windows. The closed-loop trajectories under EMPC-1 and under EMPC-2 for Case 1 are given in Figs. 4.1-4.3, the trajectories for Case 2 are given in Figs. 4.4-4.6, and the trajectories for Case 3 are given in Figs. 4.7-4.9. From Figs. 4.1-4.3, the closed-loop trajectories of the CSTR under EMPC-1 and under EMPC-2 are nearly overlapping. For this case, the PI controllers are tuned such that the control actuators respond quickly to a set-point change relative to the sampling period (and process dynamics) and thus, the control actuators are able to closely track the piecewise constant requested input trajectory $u_m(t)$ computed by EMPC. On the other hand, for Case 3 (Figs. 4.7-4.9), more differences, as expected, are observed between the closed-loop trajectories. From Fig. 4.8, EMPC-2 computes higher set-points for the actuator layer because EMPC-2 accounts for the control actuator dynamics and thus anticipates the slow response of the actuator layer by providing it a higher set-point to speed its response to the

set-point change.

Table 4.2 gives the closed-loop yield of ethylene oxide of all the simulations as well as the maximum and minimum average molar flow rate of ethylene to the reactor over each operating window, that is the minimum and maximum values of the integral:

$$\frac{1}{t_p}\int_{jt_p}^{(j+1)t_p} u_{a,1}(\tau)u_{a,2}(\tau)\ d\tau \tag{4.10}$$

over all $j \in \{0,\ 1,\ \ldots,\ 9\}$ (labeled "Min. Con." and "Max. Con." in Table 4.2, respectively). The results of Table 4.2 demonstrate that the greater the deviation of the actuator behavior from its ideal instantaneous response to an EMPC set-point change, the greater the violation of the integral constraint for EMPC-1. For example, in the case where the PI controller brings the actuator to its new set-point in only about 10% of the sampling period (Case 1), the maximum violation of the integral constraint at the end of one of the ten operating periods is about 1.15% greater than the allowable value of the integral constraint, but in the case that the actuator reaches its new set-point at the end of the sampling period (Case 3), the maximum violation of the integral constraint at the end of one of the ten operating periods is about 6.15% greater than the allowable value of the integral constraint. This discrepancy occurs because EMPC-1 only ensures that the trajectory $u_m(t)$ computed by EMPC-1 meets the integral constraint; it does not account for the effect of the actuator dynamics (i.e., the amount of material actually being fed to the CSTR). The material fed to the CSTR under EMPC-2 satisfies the integral input constraint at the end of each operating period for all three tunings presented (Table 4.2). The violation of hard constraints under EMPC-1 shows that consideration of actuators for an EMPC may be an important consideration and explicit inclusion of the actuator dynamics within the EMPC dynamic model may mitigate constraint violation.

The yield of ethylene oxide at steady-state is 6.41%; the yield under EMPC-2 is better than the steady-state yield for all cases while satisfying the integral input constraint. It is

important to point out that closed-loop yield under EMPC-1 was greater than that under EMPC-2; however, more ethylene is fed to the CSTR under EMPC-1 than the constraint value of 0.1750, which contributes to the higher yield. For example, though the closed-loop yield under EMPC-1 for Case 3 is 9.90% compared to that under EMPC-2 which was 9.41%, EMPC-1 uses significantly more ethylene than allowable (a maximum of 6.15% more than the integral constraint in an operating period). As pointed out in the "Motivating Example," accounting for the actuator layer for a system under EMPC may be important since EMPC may dictate a transient operating policy especially for the case when the actuator layer is not nearly instantaneous relative to the process dynamics. From the results in Table 4.2, as the speed of response of the actuator layer increases, the difference between closed-loop yield under EMPC-1 and EMPC-2 decreases and the amount of integral input constraint violation under EMPC-1 decreases. This implies that when the regulatory controllers are well-tuned (i.e., the actuator layer gives a fast response relative to the process dynamics), both EMPC systems give approximately the same result. Figs. 4.1-4.9 illustrate this point. Thus, these results show that for systems where actuators are known to be poorly tuned or to become poorly tuned, it is prudent to include the actuators directly within the EMPC model, especially when hard constraints are present, to avoid constraint violations.

Gaussian white noise was added to the process and actuator states of EMPC-2 using a random number generator, with zero mean and standard deviation $\sigma_w^T = [0.6 \;\; 1.2 \;\; 0.6 \;\; 0.6 \;\; 0.6 \;\; 1.8]$, and bound $\theta^T = [1.8 \;\; 3.6 \;\; 1.8 \;\; 1.8 \;\; 1.8 \;\; 3.6]$, corresponding to states $[z_1 \;\; z_2 \;\; z_3 \;\; z_4 \;\; z_5 \;\; z_6]^T$. The values of z_5 and z_6 were set to their maximum or minimum if the bounds on these states were exceeded when the noise was applied. The effect of noise was examined for the fastest PI tuning (Case 1) and the slowest PI tuning (Case 3) previously discussed. The state and input trajectories with the bounded noise applied are shown in Figs. 4.10-4.15 for these two cases.

As shown in Figs. 4.10-4.15, this realization of the process noise produces a small effect on the state and input trajectories. As a result, the average molar flow rate of ethylene to the

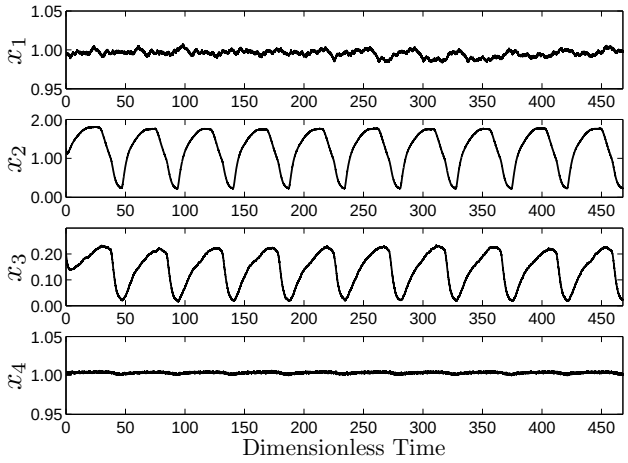

Figure 4.10: The closed-loop state trajectories of the CSTR under EMPC-2 with noise, K_c = 0.01

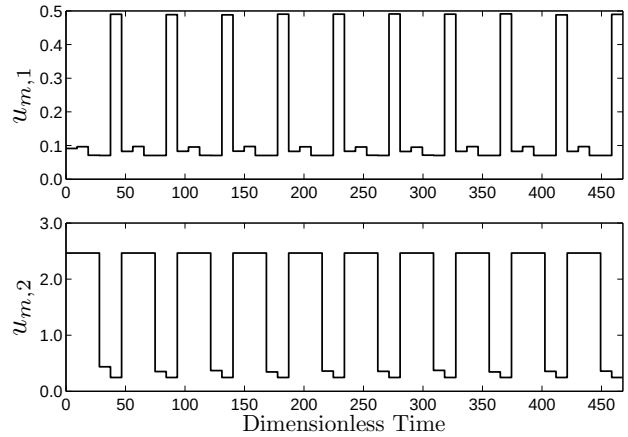

Figure 4.11: The requested input trajectory ($u_m(t)$) computed by EMPC-2 with noise, K_c = 0.01

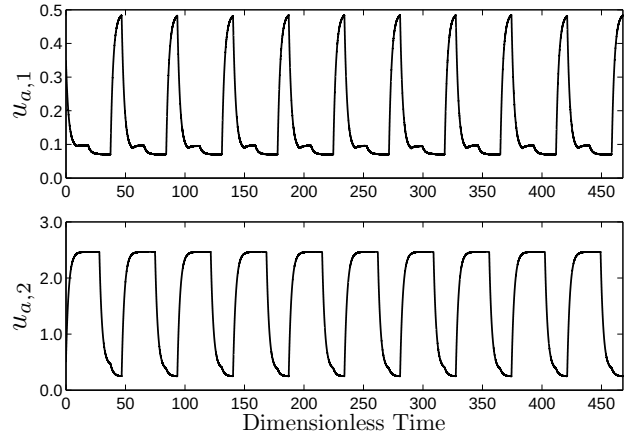

Figure 4.12: The control actuator output trajectory ($u_a(t)$) for the closed-loop CSTR under EMPC-2 with noise, $K_c = 0.01$

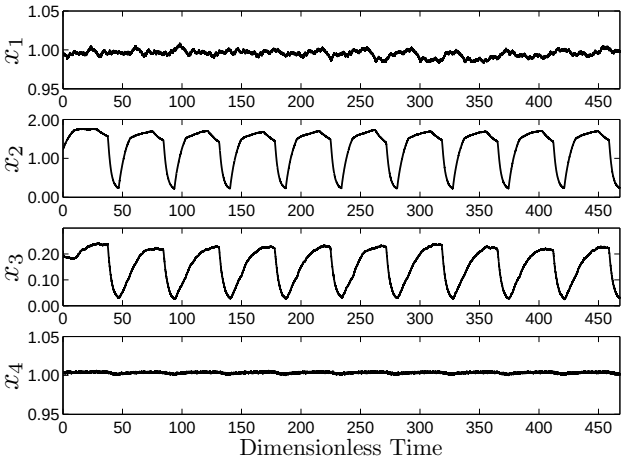

Figure 4.13: The closed-loop state trajectories of the CSTR under EMPC-2 with noise, K_c = 0.09

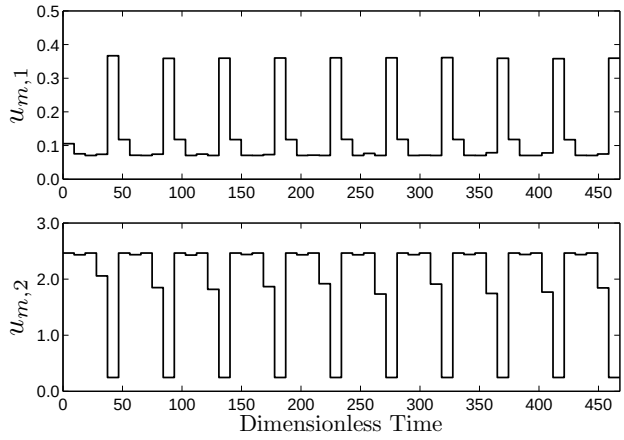

Figure 4.14: The requested input trajectory ($u_m(t)$) computed by EMPC-2 with noise, K_c = 0.09

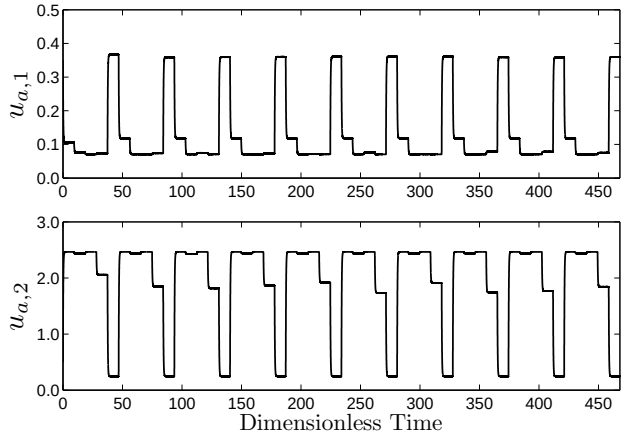

Figure 4.15: The control actuator output trajectory ($u_a(t)$) for the closed-loop CSTR under EMPC-2 with noise, $K_c = 0.09$

reactor was approximately the same for EMPC-2 with noise as it was for EMPC-2 without noise (see Table 4.2). In addition, the yield for Case 3 was approximately the same as in Table 4.2; however, a noticeable decrease in yield was observed for Case 1 in the presence of noise (yield with noise was 9.57%, which is 0.02% lower than the nominal case). Though the yield was decreased, EMPC-2 continued to meet the constraints and retain superior performance over steady-state operation in the presence of noise. These simulations also demonstrate robustness of the EMPC that incorporates the actuator dynamics.

Chapter 5

Conclusions

In this work, the control actuator dynamics were accounted for within the context of economic model predictive control (EMPC). A combined process-actuator dynamic model was developed to be used within the EMPC and Lyapunov-based constraints, imposed in the EMPC problem, were formulated on the basis of the combined process-actuator dynamic model. Conditions for closed-loop stability of the process-actuator dynamic system under the Lyapunov-based EMPC (LEMPC) were provided. Under the first mode of operation, the LEMPC optimizes the process economics while possibly operating the process system in a transient fashion, and under the second mode of operation, the LEMPC forces the state of the system to converge to a small set containing the origin. An EMPC system that accounts for the control actuator dynamics was developed and applied to a benchmark chemical process example and was compared with an EMPC system that does not account for the control actuator dynamics. From the comparison, the EMPC system that accounts for the actuator dynamics was able to satisfy an integral input constraint on the actual amount of reactant material that was being fed to the process (the EMPC system that neglected the actuator dynamics led to constraint violations) while improving closed-loop economic performance over steady-state operation.

Bibliography

[1] Marlin, T. E.; Hrymak, A. N. Real-time operations optimization of continuous processes. Proceedings of the Fifth International Conference on Chemical Process Control. Tahoe City, California, 1996; pp 156–164.

[2] Darby, M. L.; Nikolaou, M.; Jones, J.; Nicholson, D. RTO: An overview and assessment of current practice. *Journal of Process Control* **2011**, *21*, 874 – 884.

[3] Mayne, D. Q.; Rawlings, J. B.; Rao, C. V.; Scokaert, P. O. M. Constrained model predictive control: Stability and optimality. *Automatica* **2000**, *36*, 789–814.

[4] Qin, S. J.; Badgwell, T. A. A survey of industrial model predictive control technology. *Control Engineering Practice* **2003**, *11*, 733–764.

[5] Rawlings, J. B. Tutorial overview of model predictive control. *IEEE Control Systems* **2000**, *20*, 38–52.

[6] Leosirikul, A.; Chilin, D.; Liu, J.; Davis, J. F.; Christofides, P. D. Monitoring and retuning of low-level PID control loops. *Chemical Engineering Science* **2012**, *69*, 287 – 295.

[7] Ziegler, J. G.; Nichols, N. B. Optimum settings for automatic controllers. *Transactions of the ASME* **1942**, *64*.

[8] Cohen, G. H.; Coon, G. A. Theoretical consideration of retarded control. *Transactions of the ASME* **1953**, *75*, 827–834.

[9] Rivera, D. E.; Morari, M.; Skogestad, S. Internal model control: PID controller design. *Industrial & Engineering Chemistry Process Design and Development* **1986**, *25*, 252–265.

[10] Skogestad, S. Simple analytic rules for model reduction and PID controller tuning. *Journal of Process Control* **2003**, *13*, 291–309.

[11] Eriksson, P.-G.; Isaksson, A. J. Some aspects of control loop performance monitoring. Proceedings of the Third IEEE Conference on Control Applications. Glasgow, UK, 1994; pp 1029–1034.

[12] Veronesi, M.; Visioli, A. Performance assessment and retuning of PID controllers. *Industrial & Engineering Chemistry Research* **2009**, *48*, 2616–2623.

[13] Veronesi, M.; Visioli, A. Performance assessment and retuning of PID controllers for load disturbance rejection. Proceedings of the IFAC Conference on Advances in PID Control. Brescia, Italy, 2012; pp 530–535.

[14] Anderson, K. L.; Blankenship, G. L.; Lebow, L. G. A rule-based adaptive PID controller. Proceedings of the 27th IEEE Conference on Decision and Control. Austin, TX, 1988; pp 564–569.

[15] Tjønnås, J.; Johansen, T. A. Optimizing adaptive control allocation with actuator dynamics. Proceedings of the 46th IEEE Conference on Decision and Control. New Orleans, LA, 2007; pp 3780–3785.

[16] Luo, Y.; Serrani, A.; Yurkovich, S.; Doman, D. B.; Oppenheimer, M. W. Model predictive dynamic control allocation with actuator dynamics. Proceedings of the American Control Conference. Boston, MA, 2004; pp 1695–1700.

[17] Zabiri, H.; Samyudia, Y. A hybrid formulation and design of model predictive control for systems under actuator saturation and backlash. *Journal of Process Control* **2006**, *16*, 693–709.

[18] Amrit, R.; Rawlings, J. B.; Angeli, D. Economic optimization using model predictive control with a terminal cost. *Annual Reviews in Control* **2011**, *35*, 178–186.

[19] Angeli, D.; Amrit, R.; Rawlings, J. B. On average performance and stability of economic model predictive control. *IEEE Transactions on Automatic Control* **2012**, *57*, 1615–1626.

[20] Heidarinejad, M.; Liu, J.; Christofides, P. D. Economic model predictive control of nonlinear process systems using Lyapunov techniques. *AIChE Journal* **2012**, *58*, 855–870.

[21] Ellis, M.; Durand, H.; Christofides, P. D. A tutorial review of economic model predictive control methods. *Journal of Process Control* **2014**, *24*, 1156–1178.

[22] Massera, J. L. Contributions to stability theory. *Annals of Mathematics* **1956**, *64*, 182–206.

[23] Lin, Y.; Sontag, E.; Wang, Y. A smooth converse Lyapunov theorem for robust stability. *SIAM Journal on Control and Optimization* **1996**, *34*, 124–160.

[24] Khalil, H. K. *Nonlinear Systems*, 3rd ed.; Prentice Hall: Upper Saddle River, NJ, 2002.

[25] Kokotović, P.; Arcak, M. Constructive nonlinear control: a historical perspective. *Automatica* **2001**, *37*, 637–662.

[26] El-Farra, N. H.; Christofides, P. D. Bounded robust control of constrained multivariable nonlinear processes. *Chemical Engineering Science* **2003**, *58*, 3025–3047.

[27] Christofides, P. D.; El-Farra, N. H. *Control of Nonlinear and Hybrid Process Systems: Designs for Uncertainty, Constraints and Time-Delays*; Springer-Verlag: Berlin, Germany, 2005.

[28] Ellis, M.; Heidarinejad, M.; Christofides, P. D. Economic model predictive control of nonlinear singularly perturbed systems. *Journal of Process Control* **2013**, *23*, 743–754.

[29] Muñoz de la Peña, D.; Christofides, P. D. Lyapunov-based model predictive control of nonlinear systems subject to data losses. *IEEE Transactions on Automatic Control* **2008**, *53*, 2076–2089.

[30] Özgülşen, F.; Adomaitis, R. A.; Çinar, A. A numerical method for determining optimal parameter values in forced periodic operation. *Chemical Engineering Science* **1992**, *47*, 605–613.

[31] Alfani, F.; Carberry, J. J. An exploratory kinetic study of ethylene oxidation over an unmoderated supported silver catalyst. *La Chimica e L'Industria* **1970**, *52*, 1192–1196.

[32] Wächter, A.; Biegler, L. T. On the implementation of an interior-point filter line-search algorithm for large-scale nonlinear programming. *Mathematical Programming* **2006**, *106*, 25–57.